Cell Biol Toxicol (2025) 41:52
https://doi.org/10.1007/s10565-024-09980-4

RESEARCH

Molecular mechanism of ZC3H13 -mediated ferroptosis in doxorubicin resistance of triple negative breast cancer

Li Huang · Lei Han · Shuai Liang · Guohui Han

Received: 28 June 2024 / Accepted: 21 December 2024

Abstract

Background Triple negative breast cancer (TNBC) continues to be the most aggressive subtype of breast cancer that frequently develops resistance to chemotherapy. Doxorubicin (DOX) belongs to the anthracycline chemical class of the drug and is one of the widely used anticancer drugs. This study investigates the mechanism of m6A methyltransferase ZC3H13 in DOX resistance of TNBC.

Methods ZC3H13, KCNQ1OT1, and TRABD expressions in TNBC tissues or cells were detected by RT-qPCR or Western blot. The effect of ZC3H13 on DOX resistance of TNBC cells was evaluated by CCK-8, clone formation, and EdU staining. RIP was performed to analyze the enrichment of YTHDF2 or m6A on KCNQ1OT1. RIP and RNA pull-down verified the binding between KCNQ1OT1 and MLL4. The enrichment of MLL or H3K9me1/2/3 on TRABD promoter was analyzed by ChIP. A nude mouse xenograft tumor model was established to verify the mechanism in vivo.

Results ZC3H13 was poorly expressed in TNBC, and its expression further decreased in drug-resistant cells. Overexpression of ZC3H13 decreased the IC50 of drug-resistant TNBC cells to DOX, repressed proliferation, and induced ferroptosis. Mechanistically, ZC3H13-mediated m6A modification reduced the transcriptional stability of KCNQ1OT1 and inhibited its expression in a YTHDF2-dependent manner. KCNQ1OT1 enhanced the enrichment of H3K4me1/2/3 on TRABD promoter by recruiting MLL4, thus increasing TRABD expression. ZC3H13 induced ferroptosis by inhibiting KCNQ1OT1/TRABD, thereby restraining the growth of DOX-treated tumors in vivo.

Conclusion ZC3H13-mediated m6A modification reduces DOX resistance in TNBC by promoting ferroptosis via KCNQ1OT1/TRABD axis.

Keywords Triple negative breast cancer · ZC3H13 · Doxorubicin resistance · Ferroptosis · KCNQ1OT1

Introduction

Triple-negative breast cancer (TNBC) is the most aggressive subtype of breast cancer that lacks the expressions of estrogen receptor (ER), progesterone receptor (PR), and human epidermal growth factor receptor 2 (HER2) (Bai et al. 2021). Due to lack of targetable receptors, TNBC patients cannot benefit from hormone and immune-targeted therapies, and chemotherapy based on anthracycline such as doxorubicin (DOX) remains the first therapeutic option (Lev 2020).

L. Huang · L. Han · S. Liang · G. Han (✉)
Department of Breast Surgery, Shanxi Province Cancer Hospital/Shanxi Hospital Affiliated to Cancer Hospital, Shanxi Province, Chinese Academy of Medical Sciences/Cancer HospitalAffiliated to, Shanxi Medical University, Taiyuan 030013, China
e-mail: hanguohuihgh@163.com

Published online: 26 February 2025

Unfortunately, a significant proportion of TNBC patients eventually develop chemoresistance, presenting a prominent obstacle to successful treatment (Won and Spruck 2020). The development of drug resistance is resulted from multiple factors and mechanisms, such as increased cell damage repair or decreased cell death (Nedeljkovic and Damjanovic 2019). Ferroptosis, a unique form of programmed cell death induced by iron-dependent accumulation of lipid peroxides, has been reported to confer an innovative avenue to combat cancer (Wu et al. 2020b). Compelling evidence has revealed that TNBC presents a higher sensitivity to ferroptosis than other breast cancer types. Some genes or molecules related to ferroptosis exhibit characteristic expression profiles in TNBC, which are expected to become diagnostic and therapeutic targets for TNBC (Li et al. 2023). Ferroptosis can be induced by chemotherapeutic agents and profoundly reflect chemosensitivity of patients (Sha et al. 2021). Hence, deciphering ferroptosis has been acknowledged as a novel mechanism of active TNBC cell death induced by chemotherapeutic agents (Sun et al. 2021).

N6-Methyladenosine (m6A) is the most prevalent RNA epigenetic modulation in eukaryotic cells, which acts a pivotal role in diverse physiological processes including cancer pathogenesis and drug resistance (Wang et al. 2023a, 2023b). m6A modification pattern is orchestrated by methyltransferase (writer), demethylase (eraser), and RNA-binding protein (reader) (Wang et al. 2020b). As a m6A methyltransferase, zinc finger CCCH-type containing 13 (ZC3H13) expression is significantly down-regulated in TNBC tissues compared with normal tissue samples (Wang et al. 2020a). ZC3H13 is poorly expressed in ER-, PR-, basal like, and TNBC groups, and low expression of ZC3H13 predicts unfavorable prognosis in four breast cancer subtypes including luminal type A, luminal type B, HER2 enriched type, and triple negative type (Gong et al. 2020). ZC3H13 reduces DUOX1-mediated ferroptosis in laryngeal squamous cell carcinoma cells through m6A-dependent modification (Huang et al. 2023). Silence of ZC3H13 promotes ferroptosis and impairs stemness in lung adenocarcinoma cells (Jin et al. 2024). In terms of drug sensitivity, ZC3H13 has a positively association with afatinib in lung cancer (Yang et al. 2022). However, the effect and mechanism of ZC3H13 on DOX resistance in TNBC have not been reported.

m6A-modified transcripts of long noncoding RNAs (lncRNAs) are critical regulators involving in BC progression and prognosis (Yi et al. 2022; Zhang et al. 2023). LncRNA Kcnq1 overlapping transcript 1 (KCNQ1OT1) is abundantly expressed in BC, and silence of KCNQ1OT1 retards BC cell proliferation, migration and invasion in vitro and represses tumor growth in vivo (Ren et al. 2022; Wu et al. 2020a). Moreover, KCNQ1OT1 contributes to chemoresistance in osteosarcoma (Zhang et al. 2020b), hepatocellular carcinoma (Zhang et al. 2020a; Zhong et al. 2020), and small cell lung cancer (Li et al. 2021). Particularly, m6A modification of KCNQ1OT1 has been reported to regulate DOX resistance in BC via the miR-103a-3p/MDR1 axis (Zhou et al. 2023). Accordingly, the present study aims to investigate the mechanism of ZC3H13-mediated m6A modification in DOX resistance in TNBC, thereby conferring novel targets for improving the treatment and prognosis of TNBC.

Materials and methods

Ethics statement

The informed consent from all participants was obtained, and the study procedure was approved by the Ethics Committee of Shanxi Province Cancer Hospital. All animal experiment schemes were approved by the Animal Ethics Committee of Shanxi Province Cancer Hospital and implemented based on the *Guide for the Care and Use of Laboratory Animals* (Jones-Bolin 2012).

Clinical tissues

This study recruited 60 TNBC patients (38–66 years old; 47.9 ± 4.9 years old) hospitalized in Shanxi Province Cancer Hospital from May 2021 to May 2023. TNBC tissues and paracancerous normal tissues were collected and stored at −80℃. All patients were diagnosed with TNBC for the first time. Patients with a family history or previous history of malignancies and those who once received treatment were excluded.

Cell culture and treatment

Immortalized human mammary epithelial cell line MCF-10A and TNBC cell lines (MDA-MB-231, SUM-1315, BT-549, and MDA-MB-468) were purchased from ATCC (Manassas, Virginia, USA) and cultured in Roswell Park Memorial Institute (RPMI) 1640 medium supplemented with 10% fetal bovine serum (FBS), 100 μg/mL streptomycin, and 100 U/mL penicillin.

The cells were treated with increasing concentrations of DOX (0.125, 0.25, 0.5, 1, 2, 4, and 8 μg/mL) for 8 months to induce DOX-resistant human BC cells. The cells were treated with DOX at each concentration for 4 weeks, and the culture medium was changed every 3 days. The corresponding concentration of DOX was added when changing the culture medium. Dead cells sensitive to DOX were removed by centrifuging and changing the culture medium each time. DOX-resistant surviving cells were screened and collected, and treated with higher concentrations of DOX. Finally, the cells were cultured continuously at 8 μg/mL DOX for one month. After 8 months of DOX induction, the surviving cells were considered as DOX-resistant human BC cells (MDA-MB-231/ADR and MDA-MB-468/ADR). The cell culture medium was added with 8 μg/mL DOX intermittently for 24 h to maintain the DOX resistance. Moreover, 30 μg/mL DOX was used to treat DOX-resistant TNBC cells.

ZC3H13 or KCNQ1OT1 or TraB domain containing (TRABD) was subcloned to the pcDNA3.1 vector. siRNA targeting YTH-domain family member 2 (YTHDF2) was purchased from RiboBio (Guangzhou, China). The above sequences and plasmids were transfected into cells using Lipofectamine 2000 (Invitrogen, Carlsbad, CA, USA). The cells were treated with ferroptosis inhibitor ferrostatin-1 (Fer; 2 μM; MedChemExpress, Shanghai, China), with DMSO as a negative control.

Cell counting kit-8 (CCK-8) assay

CCK-8 assay was performed to detect the maximum half inhibitory concentration (IC_{50}). Briefly, the cells were seeded into 96-well plates and incubated for 48 h. The transfected cells were treated with different concentrations of DOX. Then, each well was added with 100 μL mixture of CCK-8 solution (Beyotime, Jiangsu, China) and culture medium (at a ratio of 1:9) for 2 h of incubation. The absorbance at 450 nm was measured.

Clone formation assay

The cells were seeded into 6-well plates (1×10^3 cells/well) and cultured in medium containing 10% FBS. After 2 weeks, the cells were fixed in methanol for 15 min and stained with 0.1% crystal violet. Finally, the number of colonies was recorded and counted under the microscope.

5-ethynyl-2'-deoxyuridine (EdU) staining

BeyoClick™ EdU-555 Cell Proliferation Kit (C0075S, Beyotime) was used for EdU detection. The cells were seeded into 24-well plates at a density of 5×10^4 cells/well.

Detection of iron, reactive oxygen species (ROS), and glutathione (GSH)

The iron content was determined by Iron Assay Kit (colorimetric) (ab83366, Abcam, Cambridge, MA, USA). Peroxide sensitive fluorescent probe 2'−7'-dichlorodihydrofluorescein diacetate (DCFH-DA; S0033S, Beyotime) was used for detecting the intracellular ROS level. After the indicated treatments, cells in 6-well plates were washed with phosphate-buffered saline (PBS) and incubated with 10 μM DCFH-DA for 30 min under standard conditions. The DCFH-positive cells and intracellular fluorescence were observed under the fluorescence microscope (Olympus, Tokyo, Japan) and quantified by ImageJ software (National Institutes of Health, Bethesda, MD, USA). The GSH level was detected using GSH Detection Kit (s0052, Beyotime). Briefly, TNBC cells were seeded into 6-well plates and cultured for 24 h, then harvested, and re-suspended in reagents. The absorbance at 412 nm was detected with an ultraviolet spectrophotometer (ThermoFisher Scientific, Rockford, IL, USA). The iron content, ROS level, and GSH level in tissues were also determined according to the kit instructions.

Total m6A detection and methylated RNA immunoprecipitation (MeRIP)

m6A RNA methylation Quantification Kit (colorimetric) (ab185912, Abcam) was used to detect the total m6A level of cells. Briefly, the total RNA was extracted, and 200 ng RNA was incubated with 80 μL binding buffer at 37℃ for 90 min, followed by diluted capture antibody and detection antibody. After strict cleaning, the developing agent was added, and the absorbance was measured on a microplate reader at 450 nm within 15 min. Moreover, Magna MeRIP m6A Kit (Millipore, Schwalbach, German) was used for MeRIP assay. Shortly, 5 μg of total RNA was fragmented at 70℃ for 5 min and then incubated with 3 μg m6A antibody (ab208577, Abcam) or IgG antibody (ab170190, Abcam) at 4℃ for 6 h. After washing, the enriched RNA was eluted for analysis.

RNA immunoprecipitation (RIP)

Magna RIP™ RNA Binding Protein Immunoprecipitation Kit (Millipore) was used for RIP. The cells were ice lysed in lysis buffer containing protease inhibitors and ribonuclease inhibitors for 30 min and centrifuged. The cell lysates were collected and incubated with magnetic bead protein A/G coated with control IgG antibody (ab150077, Abcam), anti-mixed linked leukemia 4 (MLL4) (pa5-116,906, ThermoFisher), and anti-YTHDF2 antibody (ab220163, Abcam) at 4℃ overnight. The RNA was extracted on the next day for detecting the relative expression.

RNA pull down

Briefly, biotin (bio)-labeled LncRNA KCNQ1OT1 was incubated with cell lysates for 2 h at 4℃. The complex was bound to streptavidin-conjugated Dynabead and then subjected to Western blot analysis to verify the enriched proteins after elution and recovery.

Actinomycin D treatment

RNA stability assay was performed as described in previous literature (Xu et al. 2022b). Briefly, the cells were treated with actinomycin D (Sigma-Aldrich, Merck KGaA, Darmstadt, Germany) at a final concentration of 5 μg/mL for 0, 3, or 6 h. Then the total RNA was extracted for RT-qPCR to quantify the relative expression of KCNQ1OT1 RNA.

Subcellular localization

Cy3-labeled KCNQ1OT1 probe and 4', 6-diamino-2-phenylindole (DAPI) were from GenePharma (Shanghai, China). FISH detection was performed using the Fluorescence In Situ Hybridization Kit (ThermoFisher Scientific), and the cellular localization was analyzed according to the manufacturer's protocol. The nuclei were counter-stained with DAPI. Images were obtained by the confocal microscope (Olympus).

PARIS™ Kit (Invitrogen, Carlsbad, CA, USA) was used for subcellular isolation assay. A total of 1×10^6 MDA-MB-231 and MDA-MB-468 cells in cell fractionation buffer were collected and centrifuged for separation of cell nucleus and cytoplasm. After removing the supernatant, the nuclei were obtained with cell lysis buffer. The isolated KCNQ1OT1 was quantified by RT-qPCR, with GAPDH as the cytoplasmic indicator and U6 as the nuclear indicator.

Chromatin immunoprecipitation (ChIP)

The ChIP procedure was performed using the EZ-ChIP Detection Kit (Millipore). The cells were collected and cross-linked with 1% formaldehyde at 37℃ for 10 min. Then, the culture medium was taken out, and the cells were suspended with cell lysate (100 μL/1×10^6) and lysed on ice for 15 min.

DNA was sheared by ultrasonication, and the chromatin fragments were incubated with anti-MLL4 (ab56770, Abcam), anti-H3K4m1 (ab176877, Abcam), anti-H3K4m3 (ab32356, Abcam) and anti-H3K4m2 (ab213224, Abcam) overnight, with IgG (ab150077, Abcam) as the negative control. Protein A/G-coupled magnetic beads (Pierce, Waltham, MA, USA) were added to capture the protein-DNA binding complex. After washing, 5 mmol/l NaCl was added for de-crosslinking and DNA was extracted. The concentration of TRABD promoter region in the complex was detected. TRABD promoter primer sequences were F: 5′-TTC CCTGATCCCGTGTTCTC-3′ and R: 5′-CTGTTC TGTGAGCCGTCAGT-3′.

Establishment and treatment of xenograft tumor in nude mice

Female BALB/c nude mice (18–20 g, 5–6 weeks old) were purchased from Shanghai SLAC Laboratory Animal Co., Ltd. (Shanghai, China) and reared under specific pathogen-free conditions. Lentiviral vectors containing ZC3H13 (Lv-ZC3H13) or Lv-KCNQ1OT1 or negative control (empty vector, Lv-NC) were synthesized by GenePharma. Further experiments were performed 48 h after lentivirus infection of cells. To establish a subcutaneous xenograft model, 2×10^6 cells were subcutaneously injected into the right armpit of mice together with 0.2 mL PBS. Two weeks after tumor transplantation, all mice were intraperitoneally injected with DOX (5 mg/kg), once every 3 days. The longest diameter (a) and shortest longitude (b) of tumors were measured with a vernier caliper, and the tumor volume was calculated (volume $= a \times b^2/2$). After 40 days, the mice were euthanized, and the tumors were excised and weighed.

Immunohistochemistry

The paraffin-embedded xenograft tumors were cut into 4-μm sections. The samples were removed from paraffin for dewaxing and rehydration before antigen extraction. Ki-67 (ab15580, Abcam) antibody was used to detect the expression of Ki-67. After incubation with the primary antibody overnight at 4℃, the sections were incubated with the secondary antibody (ab150077, Abcam) for 30 min at room temperature. The sections were stained with diaminobenzidine and counter-stained with hematoxylin. Subsequently, immunohistochemical staining images were obtained under the microscope.

Real-time quantitative polymerase chain reaction (RT-qPCR)

The total RNA was extracted using TRIzol reagent (Invitrogen) and identified using NanoDrop spectrophotometer (ThermoFisher Scientific). Reverse Transcription Kit (Promega, WI, USA) was used for RNA reverse transcription. Quantitative real-time PCR was performed using SYBR Green Kit (Promega) on the ABI7500 instrument (ThermoFisher). The primers are shown in Table 1. The relative expression of gene was calculated using the $2^{-\Delta\Delta Ct}$ method (Livak and Schmittgen 2001), with GAPDH as the internal reference.

Western blot

The total protein was extracted using radio-immunoprecipitation assay buffer (Beyotime) from cells and tissues. After adding protein loading buffer, the protein was denatured in boiling water. After centrifugation, the supernatant was collected for subsequent detection. Then, the proteins were separated by sodium dodecyl sulfate polyacrylamide gel and transferred to polyvinylidene fluoride membranes. After blocking in 5% skim milk for 2 h, the membranes were treated with primary antibodies at 4℃ overnight, including ZC3H13 (1:1000, ab314638, Abcam), MLL4 (1:500, PA5-116,906, ThermoFisher), YTHDF2 (1:1000, ab220163, Abcam), TRABD (1:1000, PA5-42,217, ThermoFisher), ACSl4 (1:10,000, ab155282, Abcam), GPX4 (1:1000, ab125066, Abcam), and FTH1 (1:500, ab75972, Abcam). After washing, the membranes were incubated with horseradish peroxidase-conjugated secondary antibody (ab205718, 1:2000, Abcam) for 1 h at room temperature. Subsequently, the enhanced chemiluminescence detection system (GE Healthcare, Aurora, OH, USA) was used to develop the bands. GAPDH (1:2500, ab9485, Abcam) was used for protein normalization. The gray scale values were

Table 1 PCR primer sequences

Gene	Sequence (5'–3')
ZC3H13	F: TTCGTACATGGCCCTTCACC
	R: CGTCTTGGCGCTTGTTCTTC
KCNQ1OT1	F: CGCTCCCATCTGCACCTTAT
	R: TTCAGCCCACTCTGAACCAC
TRABD	F: CAGCAAGAGGGACGTTGTGA
	R: CGTGCTCTCGTCCATCTTCA
YTHDF2	F: CAGGCATCAGTAGGGCAACA
	R: TTATGACCGAACCCACTGCC
GAPDH	F: GATGCTGGCGCTGAGTACG
	R: GCTAAGCAGTTGGTGGTGC

ZC3H13 zinc finger CCCH-type containing 13, *KCNQ1OT1* KCNQ1 overlapping transcript 1, *TRABD* TraB domain containing *YTHDF2* YTH-domain family member 2, *GAPDH* glyceraldehyde-3-phosphate dehydrogenase

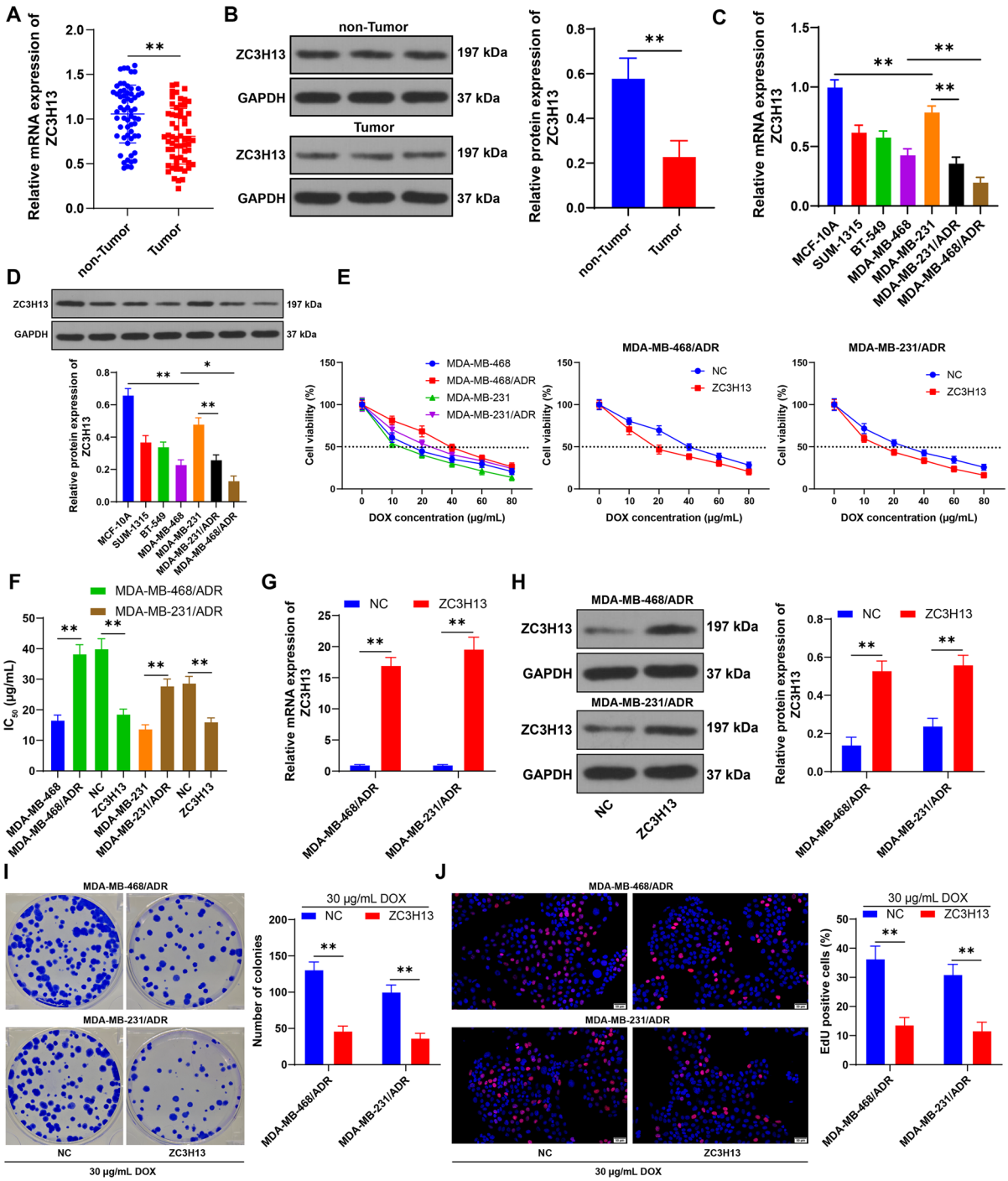
A
Relative mRNA expression of ZC3H13
non-Tumor
Tumor
B
non-Tumor
ZC3H13
GAPDH
197 kDa
37 kDa
Tumor
Relative protein expression of ZC3H13
C
Relative mRNA expression of ZC3H13
MCF-10A
SUM-1315
BT-549
MDA-MB-468
MDA-MB-231
MDA-MB-231/ADR
MDA-MB-468/ADR
D
E
Cell viability (%)
DOX concentration (μg/mL)
NC
ZC3H13
F
IC50 (μg/mL)
G
Relative mRNA expression of ZC3H13
H
I
Number of colonies
30 μg/mL DOX
J
EdU positive cells (%)

◂**Fig. 1** ZC3H13 is poorly expressed in TNBC and inhibits DOX resistance of TNBC cells. **A**-**D** ZC3H13 expression in tissues (N = 60) and cells was detected by RT-qPCR and Western blot. **E** The effect of DOX on the viability of TNBC cell lines was detected by CCK-8 assay. **F** The IC_{50} of TNBC cell lines to DOX; ZC3H13 was transfected into cells, with NC as negative control. **G**-**H** ZC3H13 expression in cells was detected by RT-qPCR and Western blot. **I**-**J** After 30 μg/mL DOX treatment, the cell proliferation ability was measured by clone formation and EdU staining assays. The cell experiments were repeated 3 times independently. Data are presented in mean ± SD. Data in panels AB were analyzed using t test; data in panels CDF were analyzed using one-way ANOVA, and data in panels EGHIJ were analyzed using two-way ANOVA, followed by Tukey's multiple comparisons test. $^{*}P < 0.05$, $^{**}P < 0.01$

measured using image J software (National Institutes of Health, Bethesda, MD, USA).

Statistical analysis

Data analysis and map plotting were performed using the SPSS 21.0 (IBM Corp., Armonk, NY, USA) and GraphPad Prism 8.0 (GraphPad Software Inc., San Diego, CA, USA). The data were examined for normal distribution and homogeneity of variance. The *t* test was adopted for comparisons between two groups, and one-way or two-way analysis of variance (ANOVA) was employed for the comparisons among multiple groups, following Tukey's multiple comparison test. A value of $P < 0.05$ indicated a significant difference.

Results

ZC3H13 is poorly expressed in TNBC and inhibits DOX resistance of TNBC cells

ZC3H13 is identified as a tumor suppressor of breast cancer (Gong et al. 2020), but its effect on DOX resistance of TNBC cells is still unclear. Compared with paracancerous tissue, the expression of ZC3H13 in cancer tissues was significantly decreased ($P < 0.01$, Fig. 1A-B). The expression of ZC3H13 was also decreased in TNBC cell lines compared with MCF-10A cells ($P < 0.01$, Fig. 1C-D). To explore the effect of ZC3H13 on the DOX resistance of TNBC cells, we selected two cell lines with higher and lower expression of ZC3H13 for drug-resistant cell construction (MDA-MB-231/ADR and MDA-MB-468/ADR) ($P < 0.01$, Fig. 1E-F), and found that the expression of ZC3H13 in drug-resistant cells was significantly lower than that in parental cells ($P < 0.05$, Fig. 1C-D). Then we up-regulated the expression of ZC3H13 in the drug-resistant cells ($P < 0.01$, Fig. 1G-H), and found that the IC_{50} of the two cell lines to DOX was significantly reduced ($P < 0.01$, Fig. 1E-F). According to the IC_{50} value of cells in each group, 30 μg/mL DOX was selected for subsequent experiments. After DOX treatment, the number of clones highly expressing ZC3H13 and EdU-positive cells were significantly diminished ($P < 0.01$, Fig. 1I-J). In short, ZC3H13 is poorly expressed in TNBC and inhibits DOX resistance of TNBC cells.

Overexpression of ZC3H13 promotes ferroptosis and then inhibits DOX resistance of TNBC cells

Targeting ferroptosis is considered a novel anti-TNBC strategy (Sun et al. 2021). Therefore, we detected the degree of ferroptosis in the two strains of cells. Overexpression of ZC3H13 led to an increase in iron ion content and ROS level in cells, while a decrease in GSH content ($P < 0.01$, Fig. 2A-C). Compared with the NC group, the expression of ferroptosis related protein ACSl4 in the ZC3H13 group was increased, while the expressions of GPX4 and FTH1 were decreased ($P < 0.01$, Fig. 2D), indicating that overexpression of ZC3H13 promoted ferroptosis in resistant TNBC cells.

To verify the effect of ferroptosis on DOX resistance in TNBC cells, we successfully inhibited the level of ferroptosis in cells overexpressing ZC3H13 through the treatment of ferroptosis inhibitor ferrostatin-1 (Fer-1) (to ensure a single variable, the DOX concentration was maintained at 30 μg/ml), leading to a decrease in the contents of iron ions and ROS, an increase in the content of GSH ($P < 0.01$, Fig. 2A-C), a decrease in the expression of ACSl4, while an increase in the expressions of GPX4 and FTH1 ($P < 0.01$, Fig. 2D). After Fer-1 treatment, the IC_{50} of cells to DOX was increased ($P < 0.01$, Fig. 2E-F), and the proliferation ability of cells was enhanced ($P < 0.01$, Fig. 2G-H). Briefly, overexpression of ZC3H13 promotes ferroptosis and then inhibits DOX resistance of TNBC cells.

ZC3H13-mediated m6A modification reduces the transcriptional stability of KCNQ1OT1 and inhibits its expression in a YTHDF2-dependent manner

ZC3H13 reduces the transcriptional stability of gene through m6A modification in the manner of YTHDF2 to inhibit the expression of gene (Xie et al. 2023). KCNQ1OT1 can be modified by m6A and is highly expressed in TNBC (Li et al. 2022; Shen et al. 2021). Our results also verified the high expression of KCNQ1OT1 in TNBC, and the expression of KCNQ1OT1 was further elevated in DOX-resistant cells ($P<0.01$, Fig. 3A-B). After overexpression of ZC3H13, the intracellular m6A level was enhanced ($P<0.01$, Fig. 3C). MeRIP was performed to further investigate the m6A modification status of KCNQ1OT1. The results unveiled that KCNQ1OT1 sequence was rich in m6A modification, and the up-regulation of ZC3H13 led to the increase of m6A modification of KCNQ1OT1 ($P<0.01$, Fig. 3D). Meanwhile, we found that the RNA stability and expression of KCNQ1OT1 were decreased with the increase of ZC3H13 expression ($P<0.01$, Fig. 3E-F). Next, we verified whether YTHDF2 affected KCNQ1OT1 expression in an m6A-dependent manner. RIP detected an increased enrichment of YTHDF2 in KCNQ1OT1 after overexpression of ZC3H13 ($P<0.01$, Fig. 3G). Subsequently, the expression of YTHDF2 in cells was decreased by transfection of siRNA ($P<0.01$, Fig. 3H-I), and the enrichment of YTHDF2 in KCNQ1OT1 was also reduced ($P<0.01$, Fig. 3G). In addition, low expression of YTHDF2 strengthened the RNA stability of KCNQ1OT1 ($P<0.05$, Fig. 3E) and elevated the expression of KCNQ1OT1 ($P<0.01$,

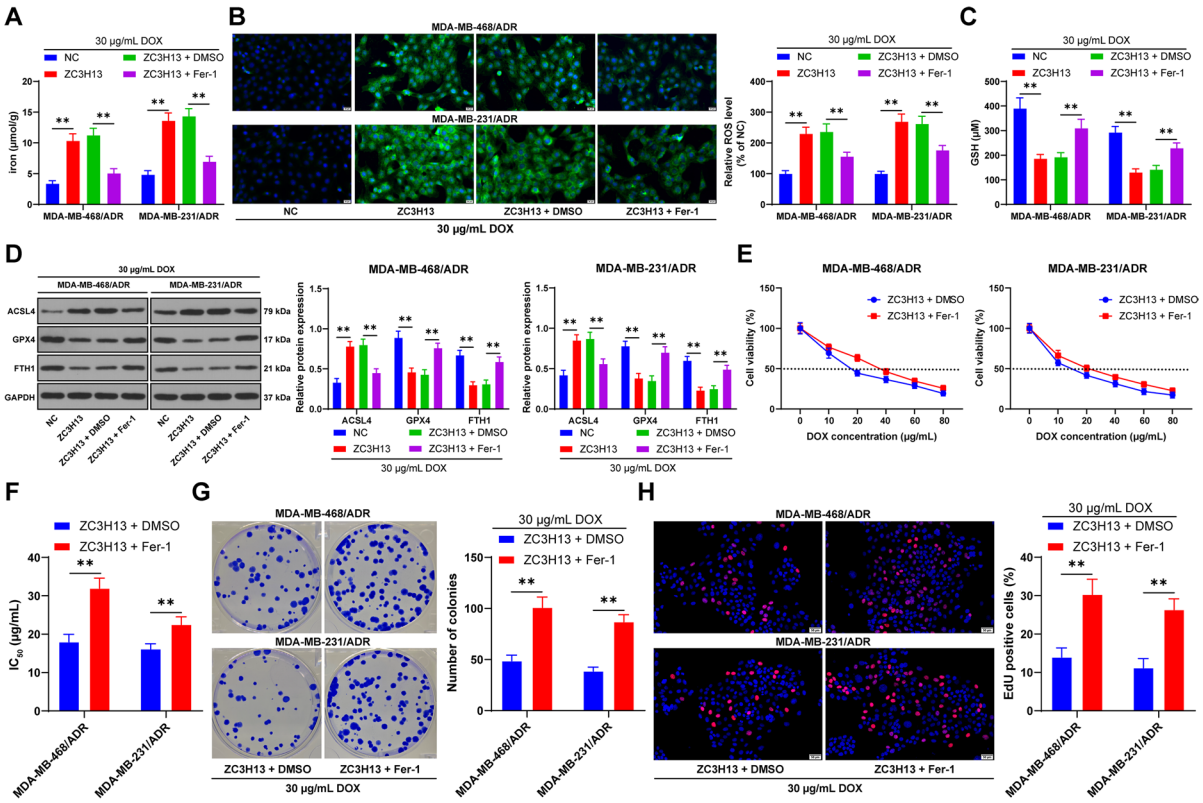

Fig. 2 Overexpression of ZC3H13 promotes ferroptosis and then inhibits DOX resistance of TNBC cells. After Fer-1 or 30 μg/mL DOX treatment, **A** the iron ion content in cells; **B** the ROS level; **C** the GSH level; **D** the protein expressions of ACSL4, GPX4, and FTH1 were detected by Western blot. **E** The effect of DOX on the viability of TNBC cell lines was detected by CCK-8 assay. **F** The IC_{50} of TNBC cell lines to DOX. **G**-**H** The cell proliferation ability was measured by clone formation and EdU staining assays. The cell experiments were repeated 3 times independently. Data are presented in mean ± SD. Data were analyzed using two-way ANOVA, followed by Tukey's multiple comparisons test. $^{**}P<0.01$

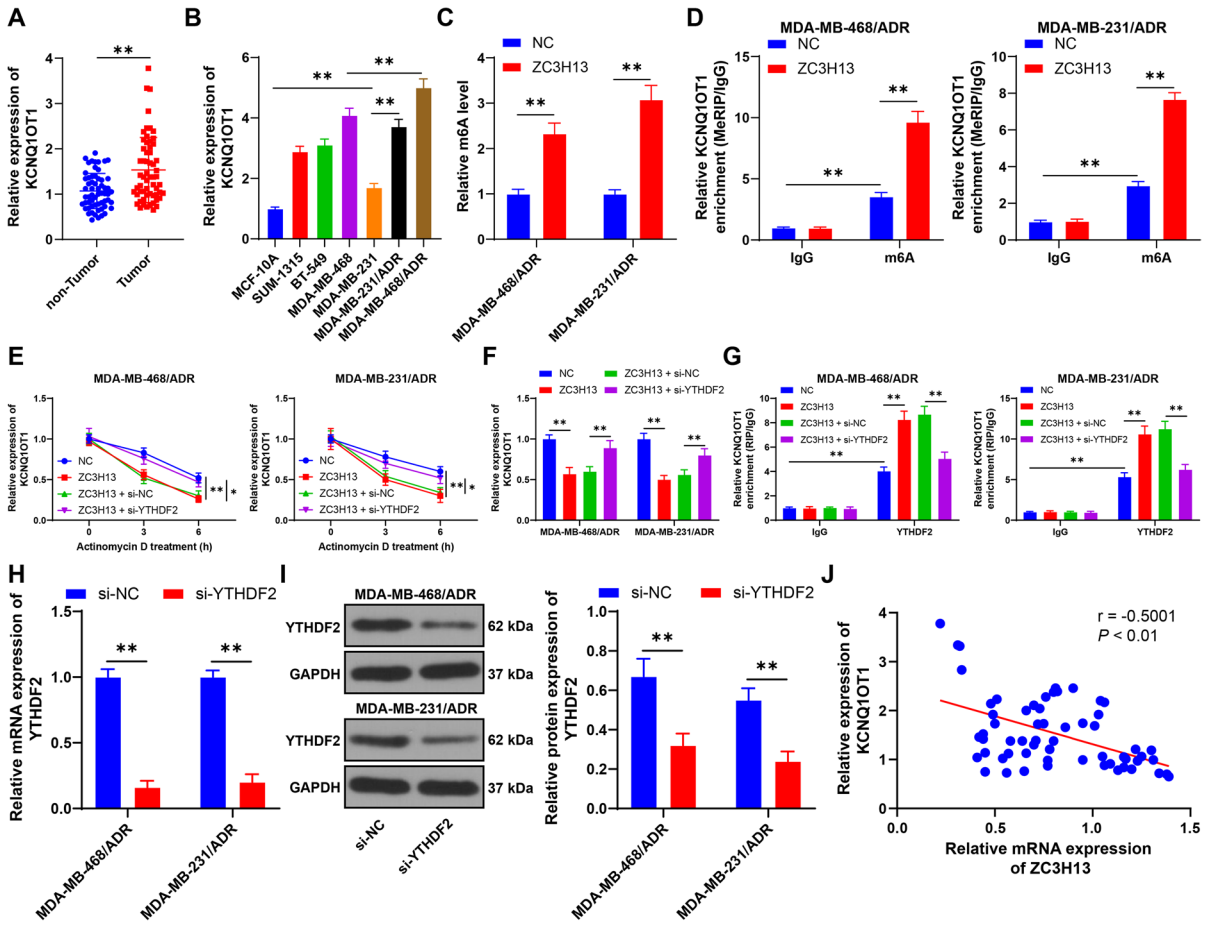

Fig. 3 ZC3H13-mediated m6A modification reduces the transcriptional stability of KCNQ1OT1 and inhibits its expression in a YTHDF2-dependent manner. **A**-**B** KCNQ1OT1 expression in tissues (N = 60) and cells was detected by RT-qPCR and Western blot. **C** The m6A level in cells was detected by m6A quantitative analysis. **D** The m6A modification of KCNQ1OT1 was analyzed by MeRIP. **E** After actinomycin D treatment, KCNQ1OT1 expression in cells was detected by RT-qPCR. **F** KCNQ1OT1 expression in cells was detected by RT-qPCR. **G** The binding between YTHDF2 and KCNQ1OT1 was analyzed by RIP. **H**-**I** YTHDF2 expression in cells after si-YTHDF2 transfection was detected by in RT-qPCR and Western blot. **J** The correlation between ZC3H13 and KCNQ1OT1 in cancer tissues was analyzed by Person correlation. The cell experiments were repeated 3 times independently. Data are presented in mean ± SD. Data in panels AB were analyzed using t test; data in panels C-I were analyzed using two-way ANOVA, followed by Tukey's multiple comparisons test. $^{*}P < 0.05$, $^{**}P < 0.01$

Fig. 3F). Moreover, ZC3H13 was negatively correlated with KCNQ1OT1 in TNBC tissues (P < 0.01, Fig. 3J). All these results indicate that ZC3H13-mediated m6A modification reduces the transcriptional stability of KCNQ1OT1 and inhibits its expression in a YTHDF2-dependent manner.

Overexpression of KCNQ1OT1 inhibits ferroptosis and alleviates the inhibitory effect of overexpression of ZC3H13 on DOX resistance in TNBC cells

We up-regulated the expression of KCNQ1OT1 in cells (P < 0.01, Fig. 4A) and performed a combined

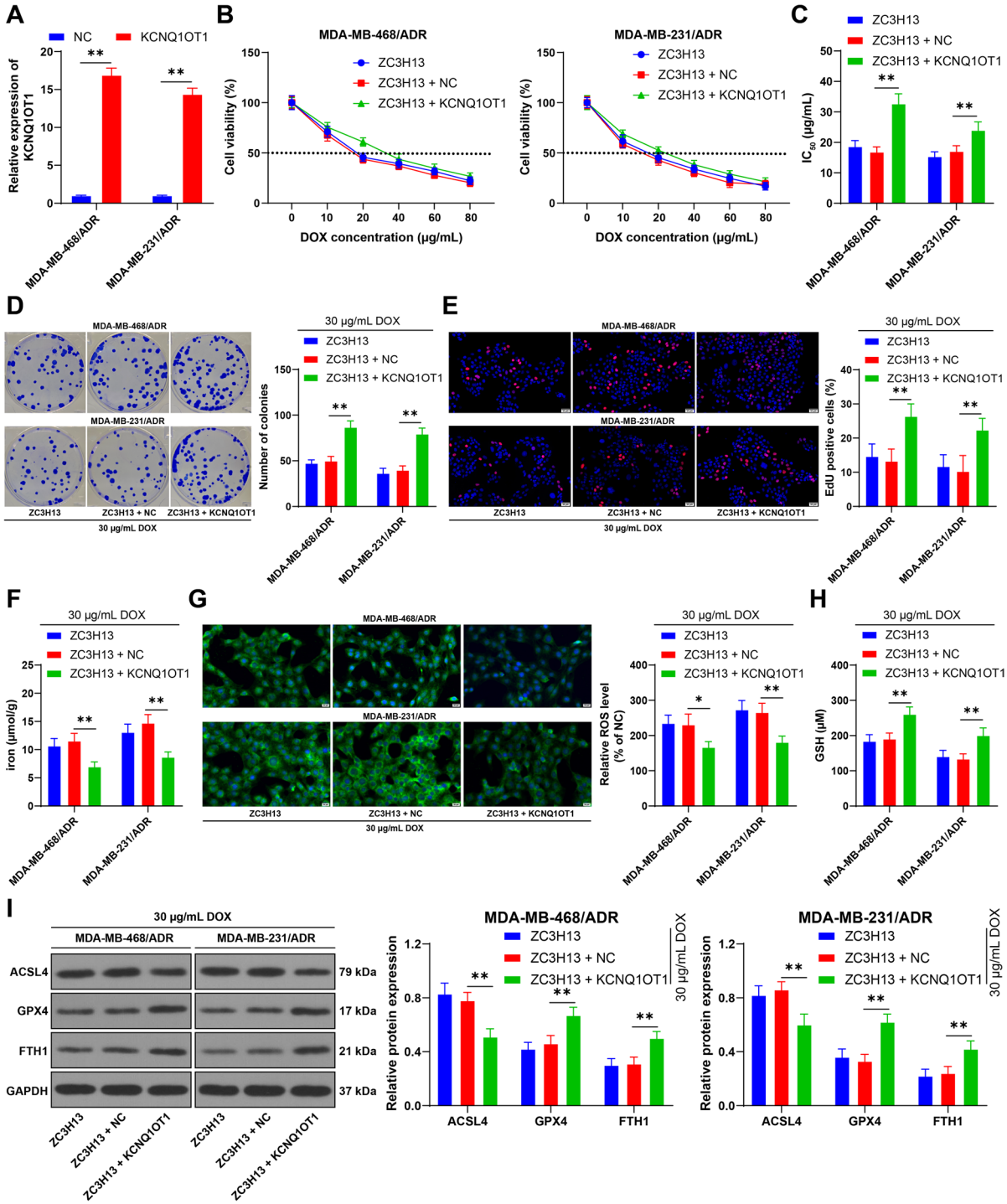

treatment with overexpression of ZC3H13, and found that the IC_{50} of cells to DOX was increased ($P < 0.01$, Fig. 4B-C). To ensure a single variable, the DOX concentration was maintained at 30 μg/mL. After DOX treatment, the proliferation ability of KCNQ1OT1-overexpressing cells was significantly strengthened ($P < 0.01$, Fig. 4D-E). In addition, compared with NC transfection, KCNQ1OT1 transfection

◂**Fig. 4** Overexpression of KCNQ1OT1 inhibits ferroptosis and alleviates the inhibitory effect of overexpression of ZC3H13 on DOX resistance in TNBC cells. KCNQ1OT1 was transfected into cells, with NC as negative control. **A** KCNQ1OT1 expression in cells was detected by RT-qPCR. **B** The effect of DOX on the viability of TNBC cell lines was detected by CCK-8 assay. **C** The IC_{50} of TNBC cell lines to DOX; after 30 μg/mL DOX treatment, **D-E** the cell proliferation ability was measured by clone formation and EdU staining assays; **F** the iron ion content in cells; **G** the ROS level; **H** the GSH level; **I** the protein expressions of ACSL4, GPX4, and FTH1 were detected by Western blot. The cell experiments were repeated 3 times independently. Data are presented in mean ± SD. Data were analyzed using two-way ANOVA, followed by Tukey's multiple comparisons test. *$P < 0.05$, **$P < 0.01$

decreased the intracellular iron ion content and ROS level, but increased the GSH content ($P < 0.05$, Fig. 4F-H). Meanwhile, we found that overexpression of KCNQ1OT1 diminished the expression of ACSl4, while elevated the expressions of GPX4 and FTH1 ($P < 0.05$, Fig. 4I). The above results suggest that overexpression of KCNQ1OT1 inhibits ferroptosis and alleviates the inhibitory effect of overexpression of ZC3H13 on DOX resistance in TNBC cells.

Nuclear localized KCNQ1OT1 interacts with MLL4 to trigger H3K4 methylation and elevate TRABD expression

The nuclear localized lncRNA SEMA3B-AS1 interacts with MLL4 to activate H3K4 methylation related transcription, thereby increasing SEMA3B expression (Chen et al. 2024). Our subcellular localization assay showed that KCNQ1OT1 was mainly localized in the nucleus of drug-resistant cells ($P < 0.01$, Fig. 5A-B). TRABD is highly expressed in TNBC (Wu et al. 2021). We also confirmed that TRABD expression was increased in TNBC cancer tissues and cell lines ($P < 0.05$, Fig. 5C-F). Next, we predicted through the RPISeq database (http://pridb.gdcb.iastate.edu/RPISeq/) (Muppirala et al. 2011) that KCNQ1OT1 has a high binding probability with MLL4 (Fig. 5G), and the binding relationship between KCNQ1OT1 and MLL4 was also verified through relevant experiments ($P < 0.01$, Fig. 5H-I). Therefore, we speculated that KCNQ1OT1 could recruit MLL4 to activate the expression of TRABD. Subsequently, ChIP analysis revealed that MLL4 and H3K4me1/2/3 were largely enriched in the TRABD promoter region, and decreased with the increase of ZC3H13 expression and increased with the increase of KCNQ1OT1 expression ($P < 0.01$, Fig. 5J). TRABD expression showed the same trend as the enrichment of MLL4 and H3K4me1/2/3 ($P < 0.01$, Fig. 5K-L). In TNBC tissues, TRABD was negatively correlated with ZC3H13 and positively correlated with KCNQ1OT1 ($P < 0.01$, Fig. 5M). Briefly, nuclear localized KCNQ1OT1 interacts with MLL4 to trigger H3K4 methylation and elevate TRABD expression.

Overexpression of TRABD inhibits ferroptosis and alleviates the inhibitory effect of overexpression of ZC3H13 on DOX resistance in TNBC cells

We up-regulated the expression of TRABD in cells ($P < 0.01$, Fig. 6A-B), followed by a combined treatment with overexpression of ZC3H13, and found that the IC_{50} of cells to DOX was increased ($P < 0.01$, Fig. 6C-D). To ensure a single variable, the DOX concentration was maintained at 30 μg/mL. After DOX treatment, the proliferation ability of TRABD-overexpressing cells was significantly enhanced ($P < 0.01$, Fig. 6E-F), and the ferroptosis level was reduced ($P < 0.05$, Fig. 6G-J). The above results show that overexpression of TRABD inhibits ferroptosis and alleviates the inhibitory effect of overexpression of ZC3H13 on DOX resistance in TNBC cells.

ZC3H13-mediated m6A modification reduces DOX resistance in TNBC by promoting ferroptosis via the KCNQ1OT1/TRABD axis

Finally, we established a nude mouse xenograft tumor model to verify our mechanism in vivo. After overexpression of ZC3H13, the tumor growth was restrained, as evidenced by the decreased tumor volume, reduced tumor weight, and decreased Ki67-positive rate, while after overexpression of KCNQ1OT1, the tumor growth was accelerated ($P < 0.05$, Fig. 7A-C). Compared with the Lv-NC group, the expression of ZC3H13 was elevated in the Lv-ZC3H13 group, while the expressions of KCNQ1OT1 and TRABD were decreased, and the m6A content was increased ($P < 0.01$, Fig. 7D-H). Compared with the Lv-ZC3H13 + Lv-NC group, the expressions of

KCNQ1OT1 and TRABD in the Lv-ZC3H13 + Lv-KCNQ1OT1 group were notably increased ($P < 0.01$, Fig. 7G-H). In addition, overexpression of ZC3H13 promoted ferroptosis in tissues, mainly manifested as increased iron ion content, ROS level, and ACSl4 expression, but decreased GSH, GPX4, and FTH1 expressions, while overexpression of KCNQ1OT1 led to the opposite trend ($P < 0.01$, Fig. 7H-K). Briefly,

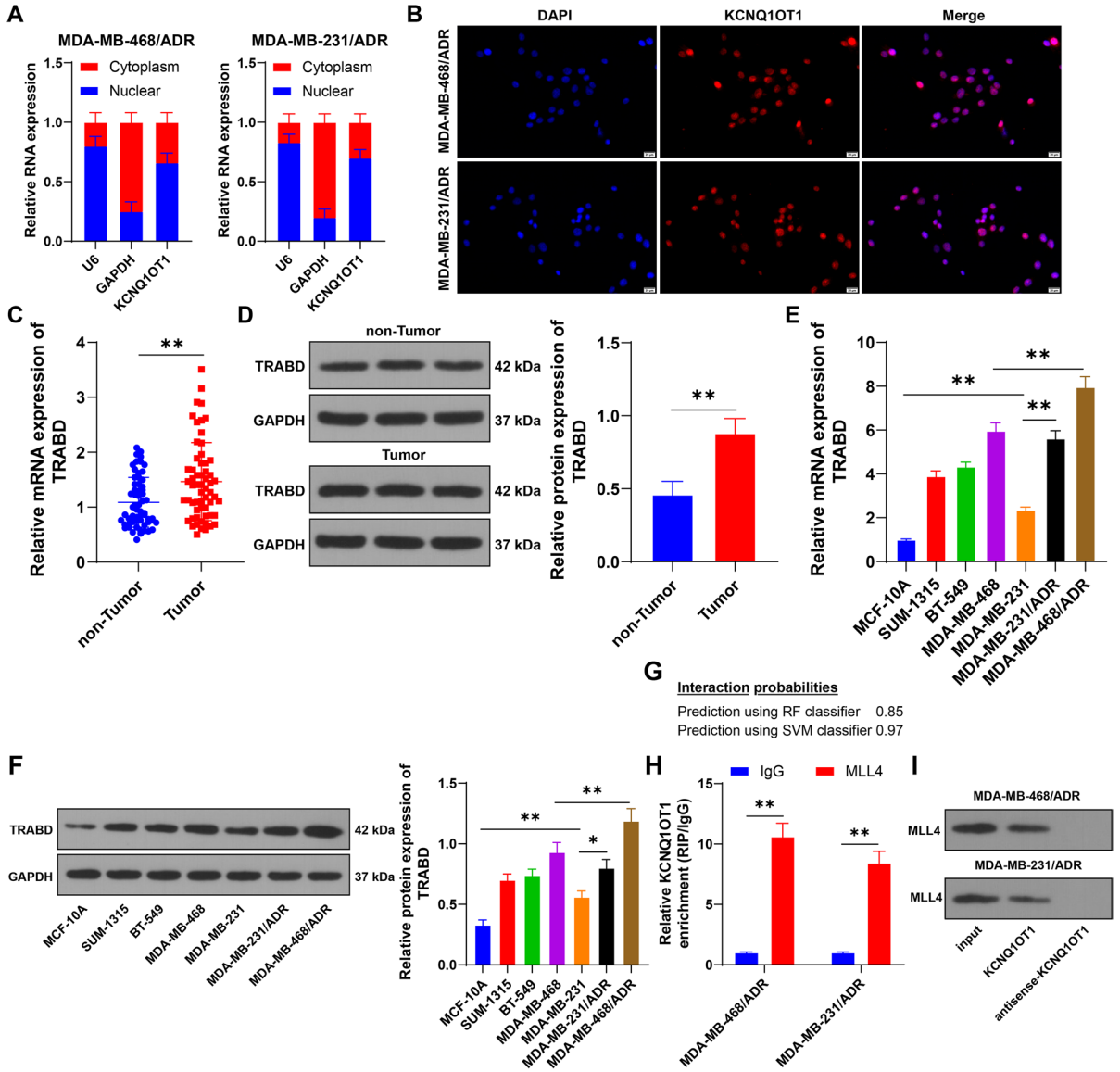

Fig. 5 Nuclear localized KCNQ1OT1 interacts with MLL4 to trigger H3K4 methylation and elevate TRABD expression. **A**-**B** The subcellular localization of KCNQ1OT1 was detected by FISH and nucleocytoplasmic fractionation assays. **C**-**F** TRABD expression in tissues (N = 60) and cells was detected by RT-qPCR and Western blot. **G** The binding probability of KCNQ1OT1 to MLL4 was predicted through the RPISeq database. **H**-**I** The binding between KCNQ1OT1 and MLL4 was analyzed by RIP and RNA pull down. **J** The enrichment of MLL4 and H3K4me1/2/3 on TRABD promoter was analyzed by ChIP. **K**-**L** TRABD expression in cells was detected by RT-qPCR and Western blot. **M** The correlation between TRABD and ZC3H13 and KCNQ1OT1 in cancer tissues was analyzed by Person correlation. The cell experiments were repeated 3 times independently. Data are presented in mean ± SD. Data in panels CD were analyzed using t test; data in panels EF were analyzed using one-way ANOVA, and data in panels HJKL were analyzed using two-way ANOVA, followed by Tukey's multiple comparisons test. $^{*}P < 0.05$, $^{**}P < 0.01$

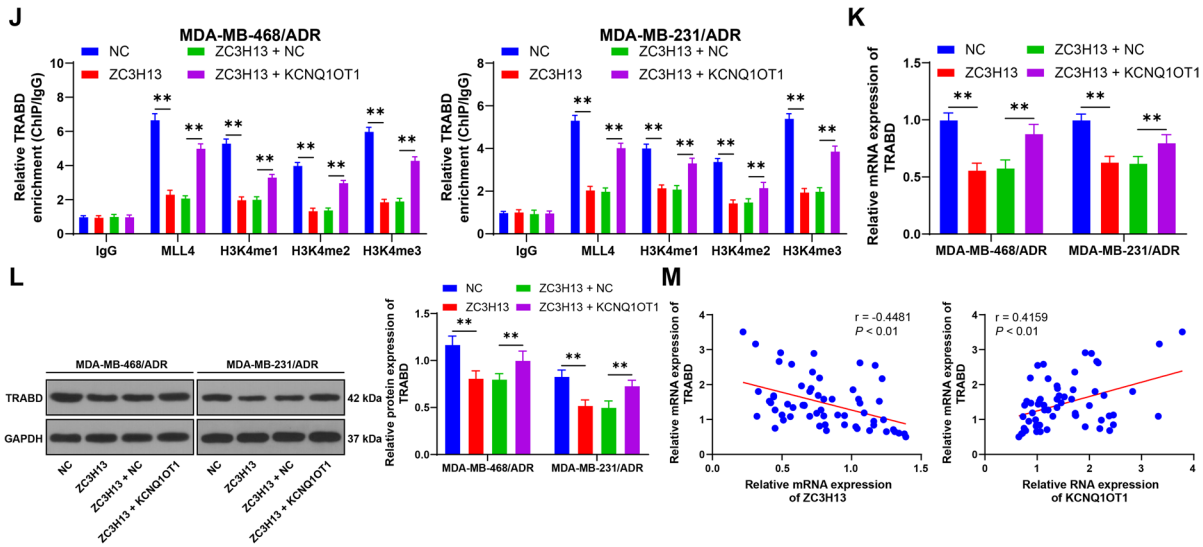

Fig. 5 (continued)

ZC3H13-mediated m6A modification reduces DOX resistance in TNBC by promoting ferroptosis via the KCNQ1OT1/TRABD axis.

Discussion

TNBC constitutes the most aggressive subtype of BC notorious for its poor prognosis, limited treatment options, and high tendency to recurrence (Derakhshan and Reis-Filho 2022). DOX is a broad-spectrum chemotherapeutic agent applied in TNBC, but DOX resistance remains an urgent clinical challenge to be solved (Kim et al. 2018). Our study reveals that ZC3H13-mediated m6A modification facilitates ferroptosis by inhibiting the KCNQ1OT1/TRABD axis and ultimately reduces DOX resistance in TNBC (Fig. 8).

m6A modification is one of the most abundant RNA modification that affects the development of drug resistance by altering the transcription stability of key genes and activating/inhibiting certain signaling pathways (Zhuang et al. 2023). ZC3H13 functions as a m6A methyltransferase and is poorly expressed in TNBC samples, and low expression of ZC3H13 leads to a decrease in m6A modification, which promotes TNBC invasion and metastasis (Gong et al. 2020). Moreover, firm links between ZC3H13-mediated m6A modification patterns and chemoresistance have been revealed in cervical cancer (Lin et al. 2022), lung cancer (Yang et al. 2022), and diffuse large B-cell lymphoma (Xu et al. 2022a). For the first time, we found that the expression of ZC3H13 in DOX-resistant cells was significantly lower than that in parental cells, and ZC3H13 attenuated DOX resistance of TNBC cells. Ferroptosis is an intracellular iron-dependent form of cell death and has been correlated with chemotherapy resistance (Zhang et al. 2022). Given that TNBC cells are rich in iron and lipids, inducing ferroptosis is a potential approach for reversing drug resistance in TNBC (Wang et al. 2023c; Wu et al. 2020b). Multiple ferroptosis-associated regulators and indicators, such as GSH, GPX4, SOD, and ACSL4, are capable of remodeling BC progression (Sui et al. 2022) and functioning as independent prognostic factors for disease-free survival (Sha et al. 2021). We overexpressed ZC3H13 in DOX-resistant TNBC cells and found that overexpression of ZC3H13 accelerated ferroptosis of TNBC-resistant cells, which was manifested by the increased iron ion content and ROS level, decreased GSH content, elevated ACSl4 expression, and reduced GPX4 and FTH1 expressions. To verify the effect of ferroptosis on DOX resistance of TNBC cells, we inhibited the increase of ferroptosis caused by overexpression of ZC3H13 by treatment with ferroptosis inhibitor Fer-1. As a result, the IC50 of TNBC cells to DOX increased and the proliferation ability enhanced.

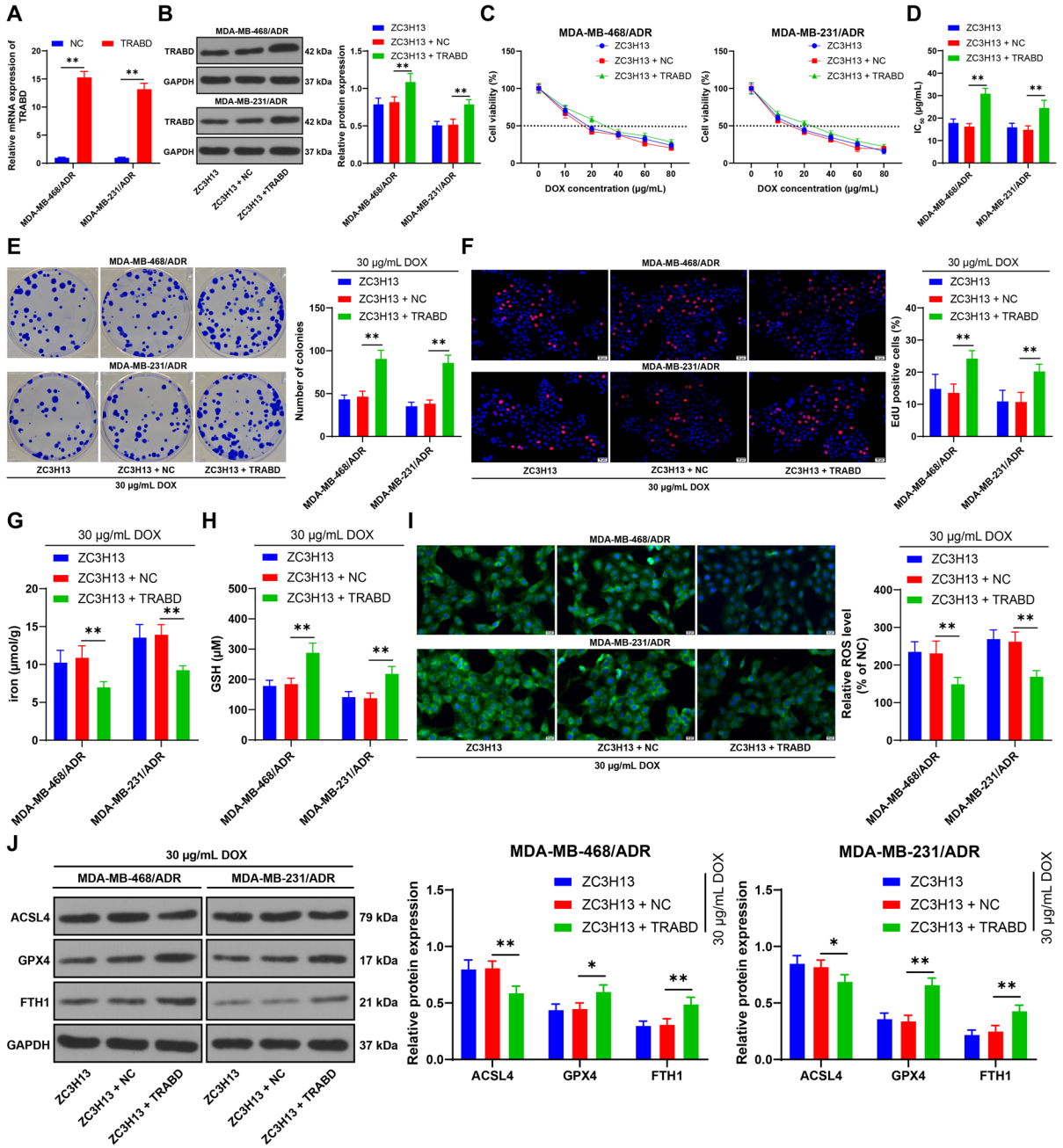

Fig. 6 Overexpression of trabd inhibits ferroptosis and alleviates the inhibitory effect of overexpression of ZC3H13 on DOX resistance in TNBC cells. TRABD was transfected into cells, with NC as negative control. **A**-**B** TRABD expression in cells was detected by RT-qPCR and Western blot. **C** The effect of DOX on the viability of TNBC cell lines was detected by CCK-8 assay. **D** The IC_{50} of TNBC cell lines to DOX. After 30 μg/mL DOX treatment, **E**–**F** the cell proliferation ability was measured by clone formation and EdU staining assays; **G** the iron ion content in cells; **H** the GSH level in cells; **I** the ROS level in cells; **J** the protein expressions of ACSL4, GPX4, and FTH1 were detected by Western blot. The cell experiments were repeated 3 times independently. Data are presented in mean ± SD. Data were analyzed using two-way ANOVA, followed by Tukey's multiple comparisons test. $^{*}P < 0.05$, $^{**}P < 0.01$

Briefly, our results suggested that overexpression of ZC3H13 repressed DOX resistance of TNBC cells by promoting ferroptosis.

LncRNAs are transcripts greater than 200 nucleotides that do not have the capacity to code proteins, which participate in the modulation of biological functions of cancers such as cancer cell proliferation/migration/invasion, cell cycle, glucose metabolism, immune evasion, and drug resistance (Feng et al. 2018). Extensive studies have revealed the aberrant

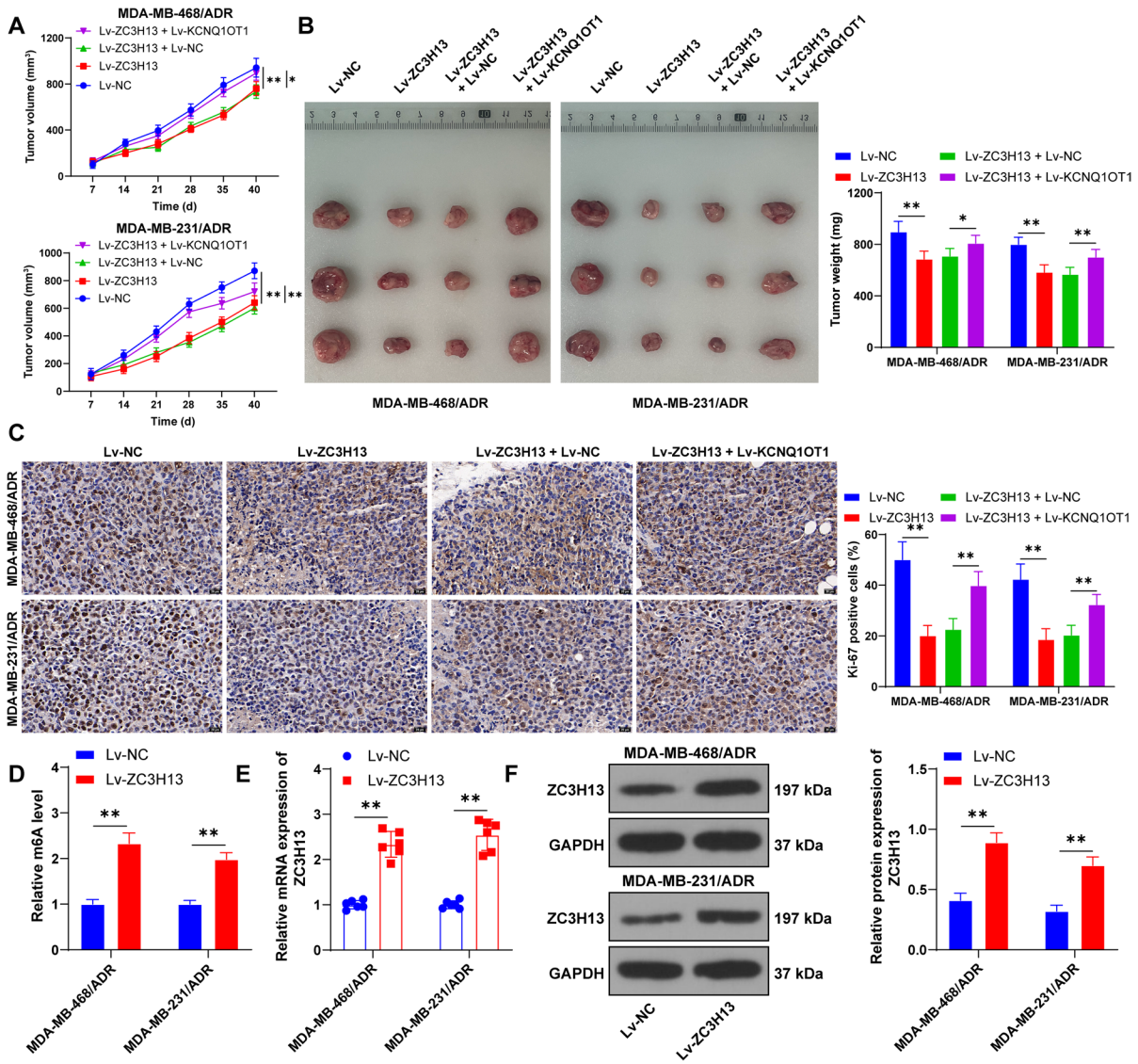

Fig. 7 ZC3H13-mediated m6A modification reduces DOX resistance in TNBC by promoting ferroptosis via the KCNQ1OT1/TRABD axis. The stably expressed drug-resistant cells were injected into nude mice, **A**-**B** the tumor volume and weight were measured (tepresentative photos of tumors). **C** The positive rate of Ki67 was detected by immunohistochemistry. **D** The m6A level in tissues was detected by m6A quantitative analysis. **E**–**F** ZC3H13 expression was detected by RT-qPCR and Western blot. **G** KCNQ1OT1 and TRABD expressions were detected by RT-qPCR. **H** The protein expressions of TRABD, ACSL4, GPX4, and FTH1 were detected by Western blot. **I** The iron ion content in tissues; **J** The ROS level in tissues; **K** The GSH level in tissues. N = 6. The cell experiments were repeated 3 times independently. Data are presented in mean ± SD. Data were analyzed using two-way ANOVA, followed by Tukey's multiple comparisons test. $^{*}P < 0.05$, $^{**}P < 0.01$

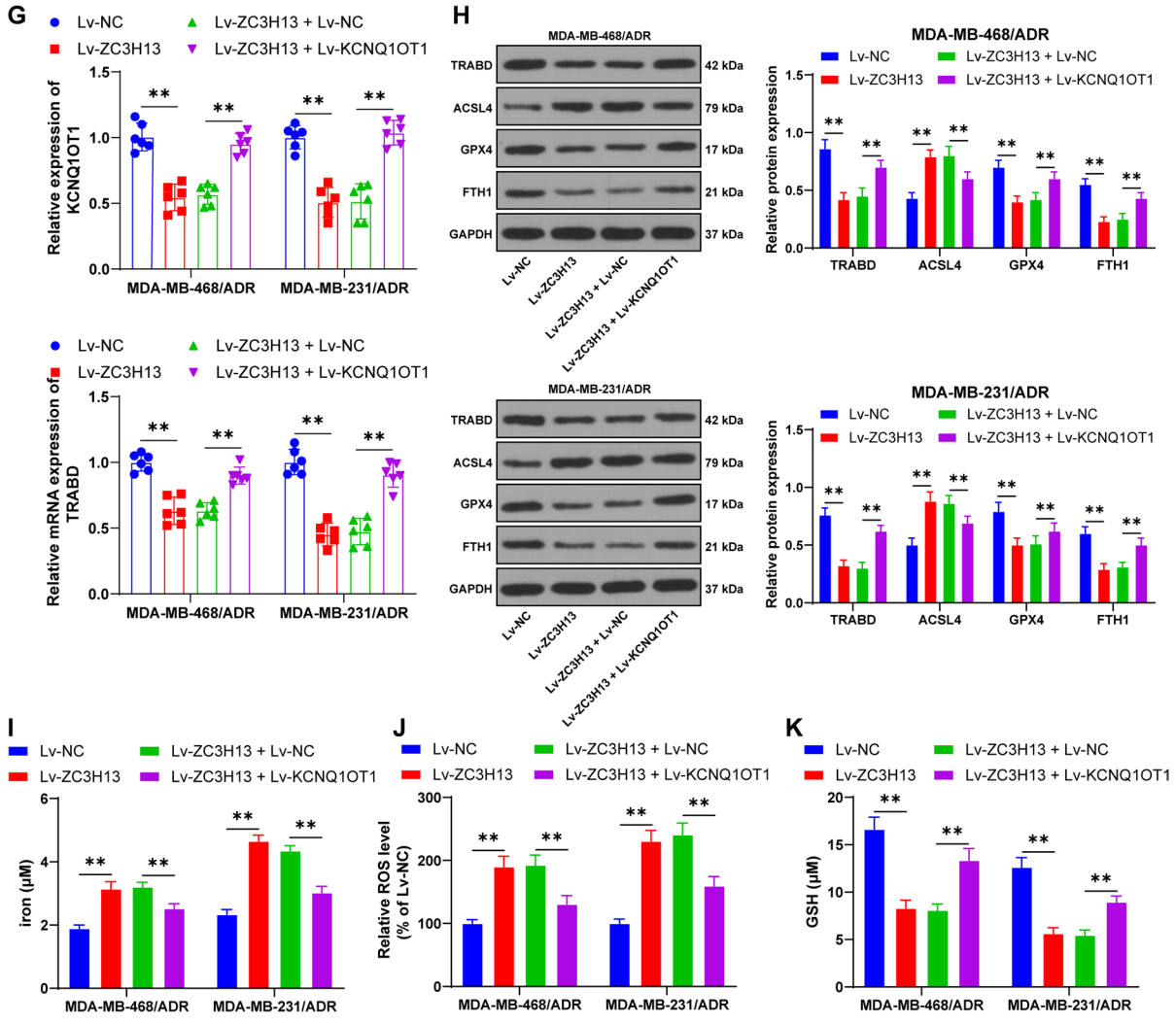

Fig. 7 (continued)

elevation of LncRNA KCNQ1OT1 expression in BC (Ren et al. 2022; Wu et al. 2020a). KCNQ1OT1 is highly expressed in TNBC, and overexpression of KCNQ1OT1 stimulates TNBC cell viability, migration, and invasion (Shen et al. 2021). Importantly, it is reported that KCNQ1OT1 can be regulated by ZC3H13-mediated m6A modification to exacerbate DOX resistance in BC (Zhou et al. 2023). Consistently, our results indicated that KCNQ1OT1 sequence was rich in m6A modification, and overexpression of ZC3H13 increased m6A modification of KCNQ1OT1. Meanwhile, the RNA stability and expression of KCNQ1OT1 decreased with the increase of ZC3H13 expression. KCNQ1OT1 is also proven to be associated with drug resistance. KCNQ1OT1 expression in chemo-insensitive tongue squamous cell carcinoma tissues is notably increased compared to chemo-sensitive tissues, and KCNQ1OT1 endows cancer cells with cisplatin-induced apoptosis resistance (Zhang et al. 2018). KCNQ1OT1 silencing not only restrains osteosarcoma cell proliferation and invasion but also, more importantly, diminishes drug resistance for 5-Fu (Zhang et al. 2020b). Consistently, we found that overexpression of KCNQ1OT1 alleviated the inhibitory effect of ZC3H13 overexpression on DOX resistance in TNBC cells. A previous study demonstrates that m6A demethylase ALKBH5 mediates KCNQ1OT1 expression

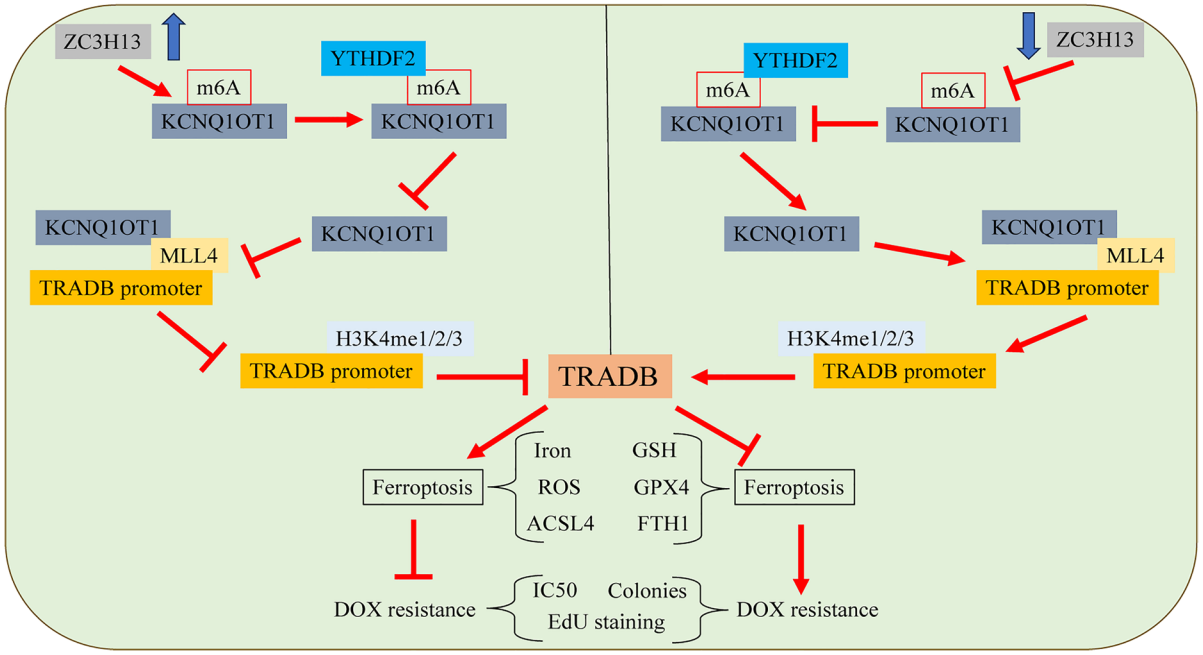

Fig. 8 ZC3H13-mediated m6A modification promotes ferroptosis and reduces DOX resistance in TNBC. ZC3H13-mediated m6A modification weakens the transcriptional stability of KCNQ1OT1 and inhibits its expression in a YTHDF2-dependent manner, thereby repressing the recruitment of MLL4 by KCNQ1OT1 and reducing the h3k4me1/2/3 enrichment on the trabd promoter, which in turn suppresses the expression of trabd, promotes ferroptosis, and ultimately reduce the DOX resistance in TNBC

via an m6A-YTHDF2-dependent manner to trigger the development of laryngeal squamous cell carcinoma (Li et al. 2022). Accordingly, we speculated whether YTHDF2 affected KCNQ1OT1 expression in an m6A-dependent manner. Our results confirmed that silence of YTHDF2 enhanced the RNA stability of KCNQ1OT1 and increased its expression. Briefly, ZC3H13-mediated m6A modification weakened the transcriptional stability of KCNQ1OT1 and suppressed its expression in a YTHDF2-dependent manner.

Further, we shifted to exploring the downstream mechanism of KCNQ1OT1. MLL4 is a specific methyltransferase of histone 3 position lysine 4 (H3K4). LncRNA SEMA3B-AS1 interacts with MLL4 to trigger H3K4 methylation-associated transcript activation and repress tumor-initiating characteristics of TNBC (Chen et al. 2024). The binding relationship between lncRNA KCNQ1OT1 and MLL4 was verified through relevant experiments, suggesting that KCNQ1OT1 might participate in regulating DOX resistance of TNBC cells by engaging in MLL4-mediated H3K4 trimethylation. ChIP analysis revealed that MLL4 and H3K4me1/2/3 were largely enriched in the TRABD promoter region, while decreased with the increase of ZC3H13 expression and increased with the increase of KCNQ1OT1 expression. The expression of TRABD showed the same trend as the enrichment of MLL4 and H3K4me1/2/3. In TNBC tissues, TRABD was negatively correlated with ZC3H13 and positively correlated with KCNQ1OT1. These results suggested that nuclear localized KCNQ1OT1 interacted with MLL4 to trigger H3K4 methylation to elevate TRABD expression. TRABD expression is increased in TNBC cells, and TRABD overexpression accelerates TNBC cell proliferation and amplifies stemness characteristics (Wu et al. 2021). Overexpression of TRABD inhibited ferroptosis and reversed the inhibitory effect of ZC3H13 overexpression on DOX resistance in TNBC cells.

To conclude, this study reports for the first time the effect and mechanism of ZC3H13 on DOX resistance

in TNBC. Mechanistically, ZC3H13-mediated m6A modification weakens the transcriptional stability of KCNQ1OT1 and represses its expression in a YTHDF2-dependent manner, thus reducing the recruitment of MLL4 by KCNQ1OT1, diminishing the enrichment of h3k4me1/2/3 on the TRABD promoter, inhibiting the expression of TRABD, and finally promoting ferroptosis to reduce the DOX resistance of TNBC.

However, this study also has several limitations. First of all, we described the role of ZC3H13 in DOX resistance in DOX-resistant cells, but failed to determine whether ZC3H13 also contributes to DOX resistance in parental TNBC cell lines. We will explore the effect and mechanism of ZC3H13 on DOX resistance in parental TNBC cells in the future. Secondly, due to funding limitation, we are unable to conduct relevant experiments to determine whether overexpressing ZC3H13 alone in DOX-resistant cells induces ferroptosis in the absence of DOX treatment. Hence, it is unclear whether ZC3H13 induces ferroptosis directly or if it merely increases sensitivity to DOX-induced ferroptosis. Thirdly, we only validated the role and mechanism of ZC3H13 in TNBC at the cellular and animal levels, but failed ro collect sufficient clinical data to analyze the correlation between the expression levels of ZC3H13, KCNQ1OT1 and TRABD and the clinical significance and prognosis of TNBC patients. Fourthly, we only explored the effect of ZC3H13 on TNBC drug resistance by promoting ferroptosis. It is unclear whether it can affect TNBC drug resistance by affecting other functions. Other types of cell death, such as apoptosis, necrosis, or autophagy, may have cross-cutting or independent effects on iron ferroptosis. In the future, we will evaluate the potential effects of ZC3H13 on other cell death pathways to ensure that other types of cell death may not be relevant or secondary to make our findings more comprehensive and accurate.

Author contributions Li Huang: Conceptualization, Data curation, Investigation, Methodology, Visualization, Writing – original draft, Writing – review & editing; Lei Han: Data curation, Investigation, Methodology, Supervision; Shuai Liang: Data curation, Formal Analysis, Validation; Guohui Han: Conceptualization, Methodology.

Funding This research did not receive any specific grant from funding agencies in the public, commercial, or not-for-profit sectors.

Data availability No datasets were generated or analysed during the current study.

Declarations

Ethics approval and consent to participate The informed consent from all participants was obtained, and the study procedure was approved by the Ethics Committee of Shanxi Province Cancer Hospital. All animal experiment schemes were approved by the Animal Ethics Committee of Shanxi Province Cancer Hospital and implemented based on the *Guide for the Care and Use of Laboratory Animals* (Jones-Bolin 2012).

Consent to publish Not applicable.

Competing interests The authors declare no competing interests.

References

Bai X, Ni J, Beretov J, Graham P, Li Y. Triple-negative breast cancer therapeutic resistance: Where is the Achilles' heel? Cancer Lett. 2021;497:100–11. https://doi.org/10.1016/j.canlet.2020.10.016

Chen D, Chen Z, Wang Z, Hong C, Wang Q, Yang P, Huang Z, Lian W, Huang Y, Fu W, Li J, Hong Z. LncRNA SEMA3B-AS1 suppresses the tumor-initiating characteristics of triple negative breast cancer via engaging in MLL4-mediated H3K4 trimethylation. Mol Carcinog. 2024;63:371–83. https://doi.org/10.1002/mc.23658

Derakhshan F, Reis-Filho JS. Pathogenesis of Triple-Negative Breast Cancer. Annu Rev Pathol. 2022;17:181–204. https://doi.org/10.1146/annurev-pathol-042420-093238.

Feng W, Wang C, Liang C, Yang H, Chen D, Yu X, Zhao W, Geng D, Li S, Chen Z, Sun M. The Dysregulated Expression of KCNQ1OT1 and Its Interaction with Downstream

Factors miR-145/CCNE2 in Breast Cancer Cells. Cell Physiol Biochem. 2018;49:432–46. https://doi.org/10.1159/000492978

Gong PJ, Shao YC, Yang Y, Song WJ, He X, Zeng YF, Huang SR, Wei L, Zhang JW. Analysis of N6-Methyladenosine Methyltransferase Reveals METTL14 and ZC3H13 as Tumor Suppressor Genes in Breast Cancer. Front Oncol. 2020;10: 578963. https://doi.org/10.3389/fonc.2020.578963

Huang L, Chen G, He J, Wang P. ZC3H13 reduced DUOX1-mediated ferroptosis in laryngeal squamous cell carcinoma cells through m6A-dependent modification. Tissue Cell. 2023;84: 102187. https://doi.org/10.1016/j.tice.2023.102187

Jin W, Sun Y, Wang J, Wang Y, Chen D, Fang M, He J, Zhong L, Ren H, Zhang Y, Yin H, Wu S, Chen R, Yan W. Arsenic trioxide suppresses lung adenocarcinoma stem cell stemness by inhibiting m6A modification to promote ferroptosis. Am J Cancer Res. 2024;14:507–25. https://doi.org/10.62347/KFAX9239

Jones-Bolin S. Guidelines for the care and use of laboratory animals in biomedical research. Curr Protoc Pharmacol. 2012;Appendix 4:Appendix 4B. https://doi.org/10.1002/0471141755.pha04bs59

Kim C, Gao R, Sei E, Brandt R, Hartman J, Hatschek T, Crosetto N, Foukakis T, Navin NE. Chemoresistance Evolution in Triple-Negative Breast Cancer Delineated by Single-Cell Sequencing. Cell. 2018;173(879–93): e13. https://doi.org/10.1016/j.cell.2018.03.041.

Lev S. Targeted therapy and drug resistance in triple-negative breast cancer: the EGFR axis. Biochem Soc Trans. 2020;48:657–65. https://doi.org/10.1042/BST20191055.

Li D, Tong Q, Lian Y, Chen Z, Zhu Y, Huang W, Wen Y, Wang Q, Liang S, Li M, Zheng J, Liu Z, Liu H, Guo L. Inhibition of lncRNA KCNQ1OT1 Improves Apoptosis and Chemotherapy Drug Response in Small Cell Lung Cancer by TGF-beta1 Mediated Epithelial-to-Mesenchymal Transition. Cancer Res Treat. 2021;53:1042–56. https://doi.org/10.4143/crt.2020.1208.

Li Y, Yan B, Wang X, Li Q, Kan X, Wang J, Sun Y, Wang P, Tian L, Liu M. ALKBH5-mediated m6A modification of lncRNA KCNQ1OT1 triggers the development of LSCC via upregulation of HOXA9. J Cell Mol Med. 2022;26:385–98. https://doi.org/10.1111/jcmm.17091.

Li J, He D, Li S, Xiao J, Zhu Z. Ferroptosis: the emerging player in remodeling triple-negative breast cancer. Front Immunol. 2023;14:1284057. https://doi.org/10.3389/fimmu.2023.1284057.

Lin X, Wang F, Chen J, Liu J, Lin YB, Li L, Chen CB, Xu Q. N(6)-methyladenosine modification of CENPK mRNA by ZC3H13 promotes cervical cancer stemness and chemoresistance. Mil Med Res. 2022;9:19. https://doi.org/10.1186/s40779-022-00378-z.

Livak KJ, Schmittgen TD. Analysis of relative gene expression data using real-time quantitative PCR and the 2(-Delta Delta C(T)) Method. Methods. 2001;25:402–8. https://doi.org/10.1006/meth.2001.1262.

Muppirala UK, Honavar VG, Dobbs D. Predicting RNA-protein interactions using only sequence information. BMC Bioinformatics. 2011;12:489. https://doi.org/10.1186/1471-2105-12-489.

Nedeljkovic M, Damjanovic A. Mechanisms of Chemotherapy Resistance in Triple-Negative Breast Cancer-How We Can Rise to the Challenge. Cells. 2019;8:957. https://doi.org/10.3390/cells8090957.

Ren Z, Xu Y, Wang X, Ren M. KCNQ1OT1 affects cell proliferation, invasion, and migration through a miR-34a / Notch3 axis in breast cancer. Environ Sci Pollut Res Int. 2022;29:28480–94. https://doi.org/10.1007/s11356-021-18434-x.

Sha R, Xu Y, Yuan C, Sheng X, Wu Z, Peng J, Wang Y, Lin Y, Zhou L, Xu S, Zhang J, Yin W, Lu J. Predictive and prognostic impact of ferroptosis-related genes ACSL4 and GPX4 on breast cancer treated with neoadjuvant chemotherapy. EBioMedicine. 2021;71: 103560. https://doi.org/10.1016/j.ebiom.2021.103560.

Shen B, Li Y, Ye Q, Qin Y. YY1-mediated long non-coding RNA Kcnq1ot1 promotes the tumor progression by regulating PTEN via DNMT1 in triple negative breast cancer. Cancer Gene Ther. 2021;28:1099–112. https://doi.org/10.1038/s41417-020-00254-9.

Sui S, Xu S, Pang D. Emerging role of ferroptosis in breast cancer: New dawn for overcoming tumor progression. Pharmacol Ther. 2022;232: 107992. https://doi.org/10.1016/j.pharmthera.2021.107992.

Sun LL, Linghu DL, Hung MC. Ferroptosis: a promising target for cancer immunotherapy. Am J Cancer Res. 2021;11:5856–63.

Wang S, Zou X, Chen Y, Cho WC, Zhou X. Effect of N6-Methyladenosine Regulators on Progression and Prognosis of Triple-Negative Breast Cancer. Front Genet. 2020a;11: 580036. https://doi.org/10.3389/fgene.2020.580036.

Wang T, Kong S, Tao M, Ju S. The potential role of RNA N6-methyladenosine in Cancer progression. Mol Cancer. 2020b;19:88. https://doi.org/10.1186/s12943-020-01204-7.

Wang C, Danli M, Yu H, Zhuo Z, Ye Z. N6-methyladenosine (m6A) as a regulator of carcinogenesis and drug resistance by targeting epithelial-mesenchymal transition and cancer stem cells. Heliyon. 2023a;9: e14001. https://doi.org/10.1016/j.heliyon.2023.e14001.

Wang D, Zhang Y, Li Q, Zhang A, Xu J, Li Y, Li W, Tang L, Yang F, Meng J. N6-methyladenosine (m6A) in cancer therapeutic resistance: Potential mechanisms and clinical implications. Biomed Pharmacother. 2023b;167: 115477. https://doi.org/10.1016/j.biopha.2023.115477.

Wang Y, Sun Y, Wang F, Wang H, Hu J. Ferroptosis induction via targeting metabolic alterations in triple-negative breast cancer. Biomed Pharmacother. 2023c;169: 115866. https://doi.org/10.1016/j.biopha.2023.115866.

Won KA, Spruck C. Triple-negative breast cancer therapy: Current and future perspectives (Review). Int J Oncol. 2020;57:1245–61. https://doi.org/10.3892/ijo.2020.5135.

Wu Y, Bi QJ, Han R, Zhang Y. Long noncoding RNA KCNQ1OT1 is correlated with human breast cancer cell development through inverse regulation of hsa-miR-107. Biochem Cell Biol. 2020a;98:338–44. https://doi.org/10.1139/bcb-2019-0271.

Wu Y, Yu C, Luo M, Cen C, Qiu J, Zhang S, Hu K. Ferroptosis in Cancer Treatment: Another Way to Rome. Front Oncol.

2020b;10: 571127. https://doi.org/10.3389/fonc.2020.571127.

Wu D, Jia H, Zhang Z, Li S. STAT3-induced HLA-F-AS1 promotes cell proliferation and stemness characteristics in triple negative breast cancer cells by upregulating TRABD. Bioorg Chem. 2021;109: 104722. https://doi.org/10.1016/j.bioorg.2021.104722.

Xie R, Chen W, Lv Y, Xu D, Huang D, Zhou T, Zhang S, Xiong C, Yu J. Overexpressed ZC3H13 suppresses papillary thyroid carcinoma growth through m6A modification-mediated IQGAP1 degradation. J Formos Med Assoc. 2023;122:738–46. https://doi.org/10.1016/j.jfma.2022.12.019.

Xu C, Liang T, Liu J, Fu Y. RAB39B as a Chemosensitivity-Related Biomarker for Diffuse Large B-Cell Lymphoma. Front Pharmacol. 2022a;13: 931501. https://doi.org/10.3389/fphar.2022.931501.

Xu Y, Lv D, Yan C, Su H, Zhang X, Shi Y, Ying K. METTL3 promotes lung adenocarcinoma tumor growth and inhibits ferroptosis by stabilizing SLC7A11 m(6)A modification. Cancer Cell Int. 2022b;22:11. https://doi.org/10.1186/s12935-021-02433-6.

Yang Y, Qian Z, Feng M, Liao W, Wu Q, Wen F, Li Q. Study on the prognosis, immune and drug resistance of m6A-related genes in lung cancer. BMC Bioinformatics. 2022;23:437. https://doi.org/10.1186/s12859-022-04984-5.

Yi D, Xu F, Wang R, Jiang C, Qin J, Lee Y, Shi X, Sang J. Deciphering the map of METTL14-mediated lncRNA m6A modification at the transcriptome-wide level in breast cancer. J Clin Lab Anal. 2022;36: e24754. https://doi.org/10.1002/jcla.24754.

Zhang S, Ma H, Zhang D, Xie S, Wang W, Li Q, Lin Z, Wang Y. LncRNA KCNQ1OT1 regulates proliferation and cisplatin resistance in tongue cancer via miR-211-5p mediated Ezrin/Fak/Src signaling. Cell Death Dis. 2018;9:742. https://doi.org/10.1038/s41419-018-0793-5.

Zhang J, Zhao X, Ma X, Yuan Z, Hu M. KCNQ1OT1 contributes to sorafenib resistance and programmed death-ligand-1-mediated immune escape via sponging miR-506 in hepatocellular carcinoma cells. Int J Mol Med. 2020a;46:1794–804. https://doi.org/10.3892/ijmm.2020.4710.

Zhang Y, Cai W, Zou Y, Zhang H. Knockdown of KCNQ1OT1 Inhibits Proliferation, Invasion, and Drug Resistance by Regulating miR-129-5p-Mediated LARP1 in Osteosarcoma. Biomed Res Int. 2020b;2020:7698767. https://doi.org/10.1155/2020/7698767.

Zhang C, Liu X, Jin S, Chen Y, Guo R. Ferroptosis in cancer therapy: a novel approach to reversing drug resistance. Mol Cancer. 2022;21:47. https://doi.org/10.1186/s12943-022-01530-y.

Zhang L, Liu C, Zhang X, Wang C, Liu D. Breast cancer prognosis and immunological characteristics are predicted using the m6A/m5C/m1A/m7G-related long noncoding RNA signature. Funct Integr Genomics. 2023;23:117. https://doi.org/10.1007/s10142-023-01026-y.

Zhong W, Dai Q, Huang Q. Effect of lncRNA KCNQ1OT1 on autophagy and drug resistance of hepatocellular carcinoma cells by targeting miR-338–3p. Cell Mol Biol (Noisy-le-grand). 2020;66:191–6

Zhou Z, Cao Y, Yang Y, Wang S, Chen F. METTL3-mediated m(6)A modification of lnc KCNQ1OT1 promotes doxorubicin resistance in breast cancer by regulating miR-103a-3p/MDR1 axis. Epigenetics. 2023;18:2217033. https://doi.org/10.1080/15592294.2023.2217033.

Zhuang H, Yu B, Tao D, Xu X, Xu Y, Wang J, Jiao Y, Wang L. The role of m6A methylation in therapy resistance in cancer. Mol Cancer. 2023;22:91. https://doi.org/10.1186/s12943-023-01782-2.